Comprehensive analysis of two different graded-index photonic-crystal lenses

Gharaati A. and Miri N.

Department of Physics, Payame Noor University, Tehran, Iran,
mirinasrin@yahoo.com

Abstract: We investigate two alternative approaches for implementing graded-index (GRIN) photonic-crystal (PC) structures that reveal a focusing effect. Gradient of the refractive index is achieved either using a symmetry-reduction approach (a structure of type I) or varying a filling fraction of PC elements (a structure of type II). We test the first structure for the frequencies located inside the first and second bands of the dispersion diagram. The focusing effect of the first structure characteristic for the frequencies located above the bandgap is stronger than that for the frequencies below the bandgap. It is demonstrated that variations of filling fractions of the elliptical air holes in the structure of type II produce a GRIN lens that manifests a pronounced focusing effect. We have also compared the focusing effects of the latter structure for the TE and TM polarizations. The both structures suggested in the present work can work in a broad enough band region.

1. Introduction

Photonic crystals (PCs) are artificial structures of which dielectric constant varies periodically along one, two or three spatial directions [1, 2]. A unique property of PCs is availability of photonic bandgaps within their photonic band structure. Due to extraordinary ability to control light propagation in a given direction, the PCs have long been a focus of many researches. The PC structures with large photonic bandgaps are promising candidates for designing waveguides [3, 4] and laser cavities [5]. Beside of this valuable aspect of the PCs, engineering photonic bands in their allowed part has given rise to a number of important optical phenomena such as negative refraction [6], super-prism effect [7, 8] and self-collimation [9, 10].

A novel kind of heterogeneous media called as graded-index (GRIN) PCs has been introduced recently to enhance possibilities for controlling the flow of light [11, 12]. GRIN PCs are a valuable choice when designing GRIN-media. They can provide any desired type of the refractive index distribution. One can design a GRIN PC structure by various structural parametric modifications, e.g. due to altering the lattice spacing, the radii of rods (or holes) and the refractive index of a material. The GRIN PCs have numerous applications when forming mode-order converters [13, 14], wavelength demultiplexers [15, 16], couplers [17] and lenses [18].

The work performed up to now has relied mostly on highly symmetric components like circular rods or holes in the PC structures. However, there is another choice for these components such as elliptical rods or holes, which are naturally anisotropic. There are two additional degrees of freedom for these structures, the orientation angle and the ellipticity. The PCs characterized by reduced symmetry that employ elliptical components have also been studied to some extent. For

instance, the imaging properties of a slab lens with elliptical rods have been analyzed with respect to the orientation angles of its elements [19]. The authors of the study [20] have demonstrated that light can be efficiently manipulated by a GRIN PC with a graded orientation of the ellipses. Moreover, a new technique has been proposed in Ref. [21] for bending a self-collimated beam, which relies on a gradual change in orientation of the elliptical rods.

The approach based on lower structural symmetry has been used in a number of optical applications. In particular, some of the earlier work has been devoted to the PCs with lower-symmetry (e.g., rectangular) geometry that induce a super-prism effect [22]. The all-angle self-collimation characteristics have been investigated in Ref. [23]. The PC structures with a parallelogram-like lattice have been explored for creating light-focusing devices associated with optical chips [24]. Moreover, the PC structures with parallelogram lattice, which are capable of working as waveguide bends with various angles, have also been investigated [25]. Some of the recent studies performed on the reduced-symmetry structures have been based on noncircular elements with a complex shape for self-collimating and designing light-manipulation effects [26, 27].

Here, we are going to explore two different PC structures both manifesting a refractive-index gradient. According to our first method, we use the symmetry-reduction approach for designing a GRIN PC structure of the type I. The second method is to vary the filling factor of the PC elements. This structure is conventionally termed as a GRIN PC structure of type II. The first approach relies upon producing a gradient of the refractive index by changing orientation of the structural elements of the PC. Since a PC is made of elliptical air holes in the dielectric background in a square lattice, a given refractive index distribution can be induced by changing gradually orientation of the elliptical holes, while the lattice constant and the filling fraction are kept intact. The resulting spatial distribution of the refractive index can be studied by plotting the effective index as a function of normalized frequency for different orientation angles [28]. Finally, we analyze the focusing effect peculiar for the GRIN PC structure of the type II for both the TE and TM polarizations.

2. System and modelling

Our main subject is investigation of the focusing effect produced by the PC structures made of elliptical air holes in a dielectric background. In order to design the GRIN PC structures with graded refractive index, two different methods have been suggested. These are the symmetry-reduction approach and varying of structural parameters of the PCs. Fig. 1 shows schematically the two PC structures with refractive index gradient, which are named respectively as the structures of types I and II. As the first step, we consider the GRIN PC structure of the type I made due to reducing symmetry of the basic unit cell. Here the elliptical elements are spatially anisotropic and have more structural degree of freedom, if compared with the rods of circular shapes.

Fig. 1. Schematic representations of GRIN PC structures of the types I (a) and II (b). The both structures are composed of elliptical air holes made in dielectric background.

The PC under study is composed of a square array of air holes in a silicium background with the permittivity equal to $\varepsilon = (3.46)^2$. The array includes 12 columns and 21 rows. Let the major and minor radii of the elliptical air holes shown in Fig. 2a be r_1 and r_2, respectively. It is known that any change in the symmetry of the basic lattice, or in the shape and the orientation of the dielectric elements, must affect the dispersion diagrams [29]. We choose the orientation angles θ (i.e., the angle between the major axis of the elliptical air hole and the *x* axis – see Fig. 2a) to be equal to 0 and 90 deg when calculating the band structure. The plane-wave expansion method has been employed for plotting the dispersion diagrams. Fig. 2b shows the band structure diagrams for the perfect PCs in which the ellipses are rotated by the angles 0 and 90 deg. In contrast to the PCs with circular elements, for which one can consider only the irreducible Brillouin zone (i.e., a one eighth of the first zone) in the dispersion diagrams, in case of the PCs with elliptical elements we have to scrutinize a one-fourth of the first Brillouin zone. The photonic band diagrams plotted in Fig. 2b correspond to the X1ΓXM direction, the TM polarization, and the orientation angles $\theta = 0$ and $\theta = 90$ deg. As evident from Fig. 2b, the photonic bands are not the same for the ΓX and ΓX1 directions, which is a result of anisotropic characteristics of the ellipses.

The group index can be defined as $n_g = c / \nabla_k \omega(k)$, where *c* is the light velocity in vacuum, ∇_k the gradient operator with respect to the wave vector *k*, and ω the angular frequency. The group index referred hereafter to as an effective refractive index n_{eff}, can be derived from the band-structure diagram. We have calculated the effective refractive index for the first TM band along the ΓX direction for the PCs with the elliptical air holes, in which the ellipses are rotated by 0 and 90 deg. As seen from Fig. 2c, changes in the orientation of the elliptical holes can produce notable index variations, even if the filling fractions are kept invariable. Moreover, different index gradients can be generated since the effective refractive index depends on the θ value. Note that the r_1 and r_2 values taken in our calculations are 0.4*a* and 0.2*a* (with *a* being the lattice spacing), so that the ellipticity *e* is equal to 0.5. We limit our study to the case of TM polarization of which electric field is parallel to the segment axis.
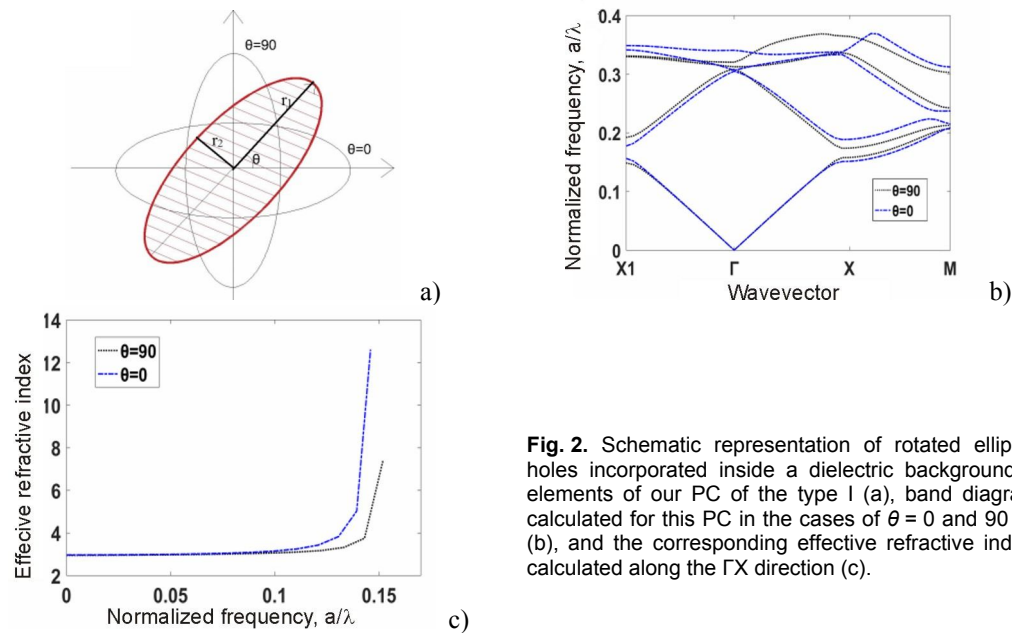

a)

b)

c)

Fig. 2. Schematic representation of rotated elliptical holes incorporated inside a dielectric background as elements of our PC of the type I (a), band diagrams calculated for this PC in the cases of $\theta = 0$ and 90 deg (b), and the corresponding effective refractive indices calculated along the ΓX direction (c).

Afterwards, a finite-difference time-domain analysis has been conducted to obtain the transmission spectra over a wide enough bandwidth (see Fig. 3). As expected, one observes a transmission window and a bandgap. This is because the relevant characteristics are kept unchanged along the propagation direction and only a transverse index gradient is available.

To study a focusing capability of our GRIN PC lens in our simulations, we have used a pulse with the Gaussian profile at different normalized frequencies $a/\lambda = 0.09$, 0.10, 0.20 and 0.21. This frequency range covers both the first and the second bands. The patterns corresponding to electric field propagation through the structure are displayed in Fig. 4. Starting from the value $a/\lambda = 0.20$ located in the second band of the diagram, the structure reveals strong focusing. The latter effect becomes still more pronounced for the frequency 0.21. For the two other frequencies located in the first band, 0.09 and 0.10, the structure shows a moderate focusing effect. From the results obtained one can conclude that the GRIN PC produced according to the low-symmetry approach works properly as an optical lens.
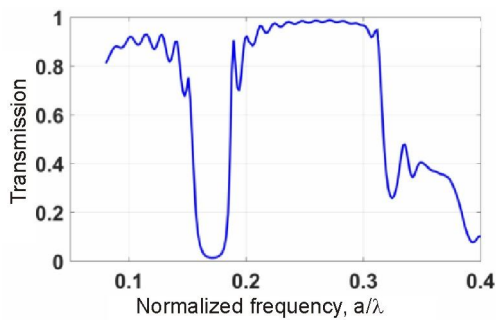
Fig. 3. Transmission spectrum calculated for the PC structure of the type I made of rotated elliptical air holes.
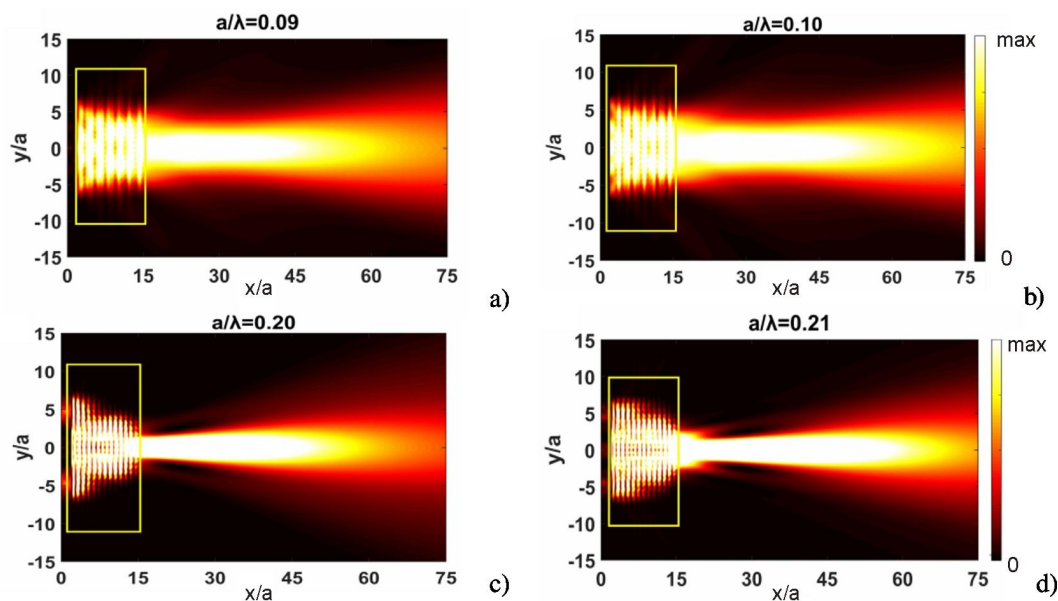
Fig. 4. Spatial field distributions calculated for the GRIN PC structure of the type I at different normalized frequencies: 0.09 (a), 0.10 (b), 0.20 (c) and 0.21 (d). A rectangular box corresponds to the GRIN PC structure itself.

To analyze our results more precisely, we have plotted in Fig. 5 the field intensity at the focal point at the output of the GRIN PC. The full width at half maximum (FWHM) values

corresponding to the four different frequencies presented in Fig. 5a are equal to $7.5a$, $7.4a$, $3.43a$ and $3.35a$ in terms of the lattice constant. The same parameters are equal to 0.75λ, 0.67λ, 0.72λ and 0.67λ in terms of the light wavelength. The above results demonstrate that the PC structure of the type I manifests a notable focusing effect for the input beams with the frequencies located above the bandgap but not for the frequencies lower than the bandgap.
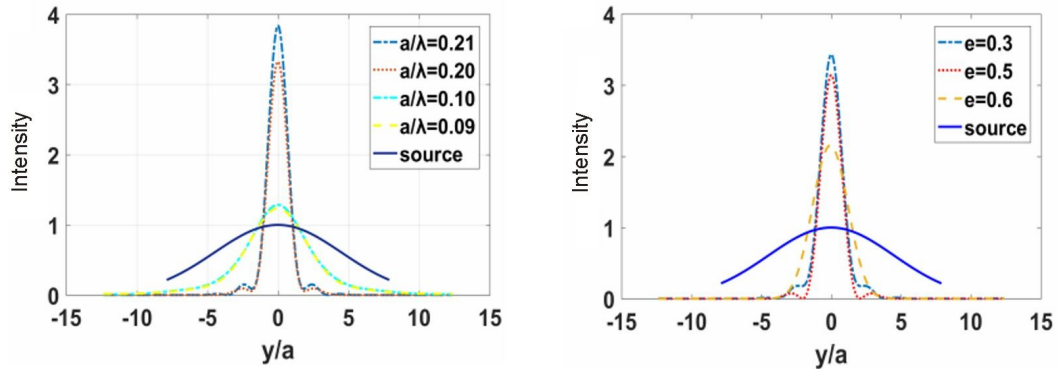

Fig. 5. Cross-section field profiles calculated for the normalized frequencies 0.21, 0.20, 0.10 and 0.09 (a) and the ellipticity values 0.3, 0.5 and 0.6 (b).

For the case of $a/\lambda = 0.20$, we have also investigated the focusing characteristics of the GRIN PC depending on the ellipticity ($e = 0.3$, 0.5 and 0.6). Light with the unit amplitude passes through the GRIN lens and is focused into a small area. This means that the FWHM decreases, whereas the field intensity increases and becomes greater than unity. Fig. 5b presents the cross-sectional profiles of the outgoing wave field at the focal point, as calculated for the structures with different ellipticities. It is obvious that the ellipticity increase from 0.5 to 0.6 decreases the field intensity at the focal point. In contrast, decreasing ellipticity induces a stronger focusing effect and increases the field intensity at the focal point. In other words, in the case of small ellipticities the effective refractive index increases more sharply from the edges of the GRIN PC structure of the type I towards its centre, thus increasing the field intensity at the focal point.

Now we study how the refractive index of the background material and the ellipticity of the elliptical holes affect the transmission spectrum for the structure of the type I (see Fig. 6). With increasing refractive index, the reflectance gap gets narrower and moves towards longer wavelengths. When the ellipticity increases, the reflectance gap shifts towards shorter wavelengths and the gap becomes wider. As a consequence, one can control the location of the reflectance gap by adjusting the background material and the ellipticity. Therefore, our PC lens manifests a tunable reflectance gap that can easily be shifted by changing either the background material or the ellipticity.

Now we proceed to study focusing for the GRIN PC structure of the type II (see Fig. 1b). We remind that this structure is designed such that the filling fraction is altered along the direction normal to the propagation direction. Here unmodified PC structure is composed of a square array of elliptical air holes in a dielectric substrate with the permittivity $\varepsilon = (2.00)^2$, with 12 columns and 21 rows as before. Again, the major and minor radii of the elliptical holes are respectively r_1 and r_2. The latter parameters are selected such that the ellipticity be the same as before ($e = 0.5$). Hereafter, the major radii of the elliptical holes vary from $0.45a$ to $0.10a$, while the minor radii are defined as $0.5r_1$ for each row of the PC structures.

As the first stage, we have employed the standard plane-wave expansion technique for calculating dispersion diagram of the PC structures characterized with different radii of the elliptical holes. The structures of the first band in the ΓX direction are presented in Fig. 7a. When the hole radii increase along the direction y, the bands move towards higher frequencies. The effective refractive index corresponding to each dispersion curve has been calculated issuing from the slope of each band (see Fig. 7b).
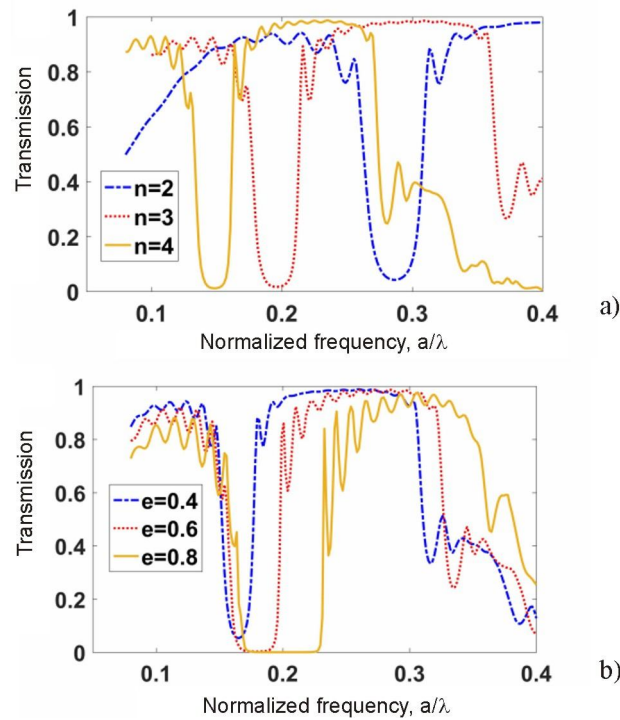

Fig. 6. Transmission spectra calculated for different refractive indices of the background material (a) and different ellipticities (b).
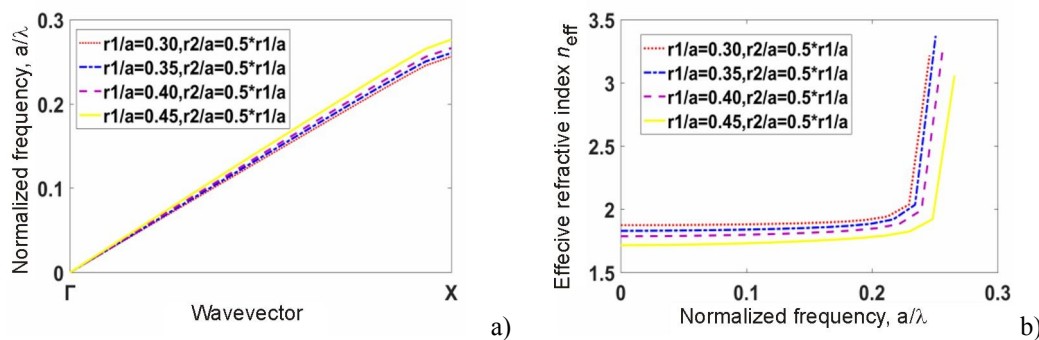

Fig. 7. Band diagrams for the PC with elliptical holes in which the filling fractions are altered (a), and the corresponding dependences of effective refractive index on the normalized frequency along the ΓX direction (b).

Next, the finite-difference time-domain method has been applied to model numerically the light propagation through the GRIN PC structure. It is suggested that the domain under computation is surrounded by a perfectly matched layer. To be more specific, we choose the polarization TM as a main subject of our numerical simulations. Afterwards, we will compare the

main results with those obtained for the TE polarization. Fig. 8 displays the electric field distributions calculated for the PC structure at different frequencies $a/\lambda = 0.13$, 0.18 and 0.23. It is clear that the GRIN PC structure of the type II reveals a strong focusing effect. We have also calculated the associated field intensities. As seen from Fig 9a, increase in the normalized frequency of the input beam increases the peak of the field intensity. The distance between the end face of the GRIN structure and the focal point amount to $8.2a$, $5.7a$ and $3.2a$ for the three different frequencies. The FWHM values for each of those cases are equal to 0.9λ, 0.82λ and 0.7λ. Our results demonstrate that the GRIN PC structure of the type II can function as a compact focusing lens with a broad bandwidth.

As mentioned above, the data obtained thus far for the GRIN PC structure of the type II refers to the ellipticity $e = 0.5$. Now we report on the focusing features of our structure depending on the ellipticity, taking the values $e = 0.3$, 0.5 and 0.8 as examples. Notice that the normalized frequency is now fixed at 0.23. Fig. 9b shows the cross-sectional profiles of the electric field that corresponds to the waves emergent from the structures with different ellipticities. When the ellipticity increases, the peak of the field intensity reaches higher values. This is caused by the fact that increasing ellipticity reduces the refractive index at the edges of the structure if compared to its centre. Then the effective refractive index increases at the centre of the structure. Therefore, the outgoing wave becomes more 'concentrated' with increasing ellipticity, whereas the field intensity at the focal point increases. The FWHM values calculated for the three cases under study are equal to 1.19λ, 0.94λ and 0.74λ. The structure with the ellipticity $e = 0.8$ reveals the lowest FWHM.
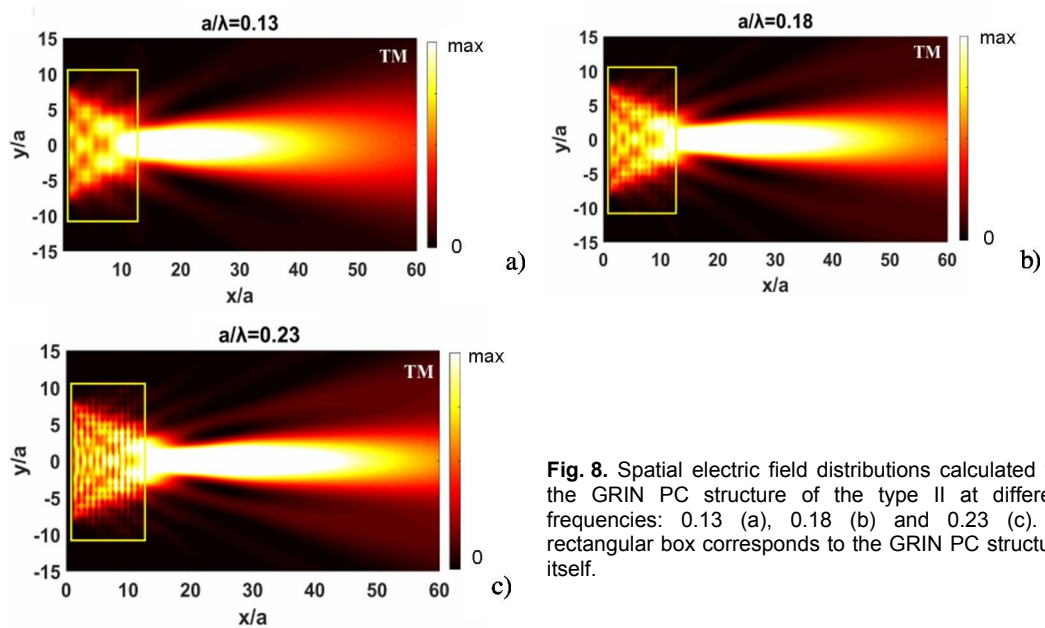

Fig. 8. Spatial electric field distributions calculated for the GRIN PC structure of the type II at different frequencies: 0.13 (a), 0.18 (b) and 0.23 (c). A rectangular box corresponds to the GRIN PC structure itself.

For a comparison, we have also calculated the focusing characteristics of our structure of the type II for the case of TE polarization. The transmission spectra obtained for the TE and TM polarizations are plotted in Fig. 10. Surprisingly enough, the transmission spectra for the both polarizations are nearly coincident. The windows of high optical transmission correspond to the frequency intervals $a/\lambda = 0.15–0.17$ and $0.23–0.30$ for the TM polarization and $a/\lambda = 0.13–0.17$ and $0.22–0.30$ for the TE polarization.
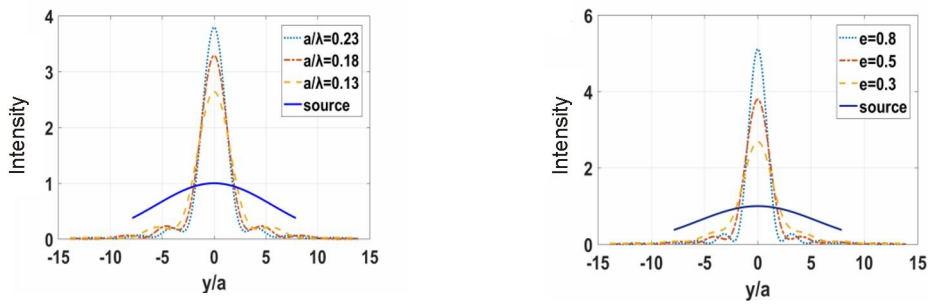
Fig. 9. Cross-section profiles of electric field calculated at the focal point of our GRIN PC structure of the type II for different frequencies (a) and different ellipticity values (b).
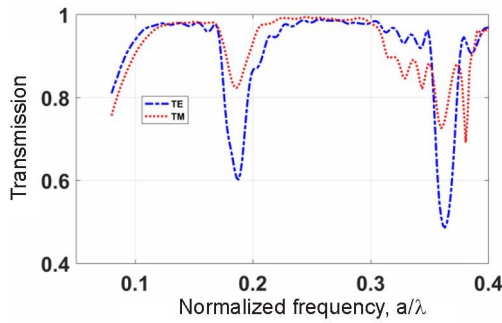

Fig. 10. Transmission spectra of our GRIN PC structure of the type II calculated for the TE and TM polarizations.

Fig. 11 shows the output electric-field distributions for the GRIN PC structure of the type II, as obtained in the case of TE polarization. It is evident that the outgoing beam becomes more confined with increasing normalized frequency of the input beam. To provide a more accurate comparison of the focusing effects achieved for the TE and TM polarization, we have plotted in Fig. 12 the cross-sectional field intensity profiles at the focal point for the both polarizations. In the case of TE polarization, the distances between the end face of the GRIN structure and the focal point are equal to $6.0a$, $5.05a$ and $2.55a$ at the three different frequencies analyzed by us. In all of the cases, the ellipticity is taken to be equal to 0.5 for the both polarizations.
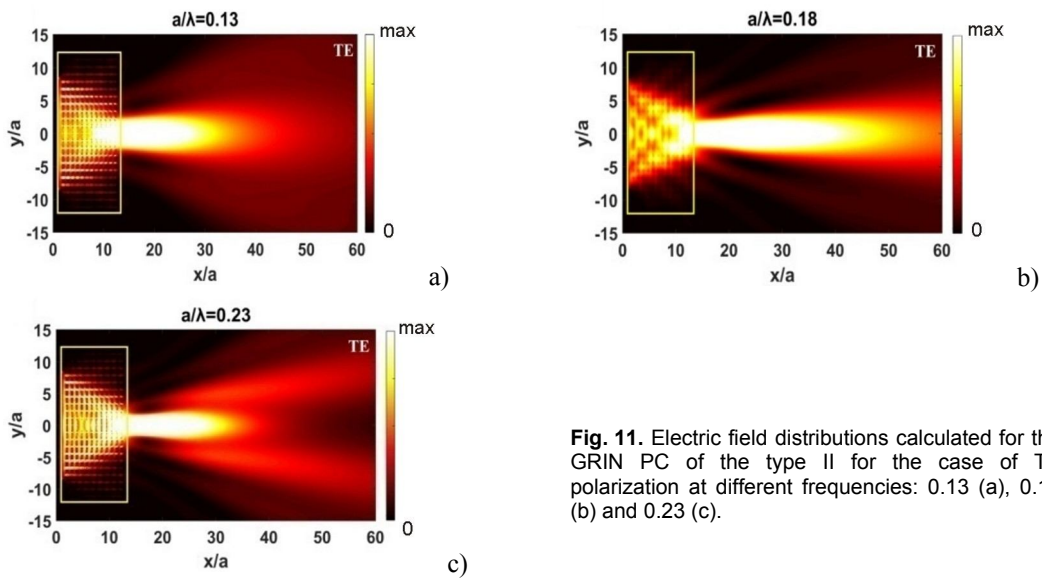

Fig. 11. Electric field distributions calculated for the GRIN PC of the type II for the case of TE polarization at different frequencies: 0.13 (a), 0.18 (b) and 0.23 (c).
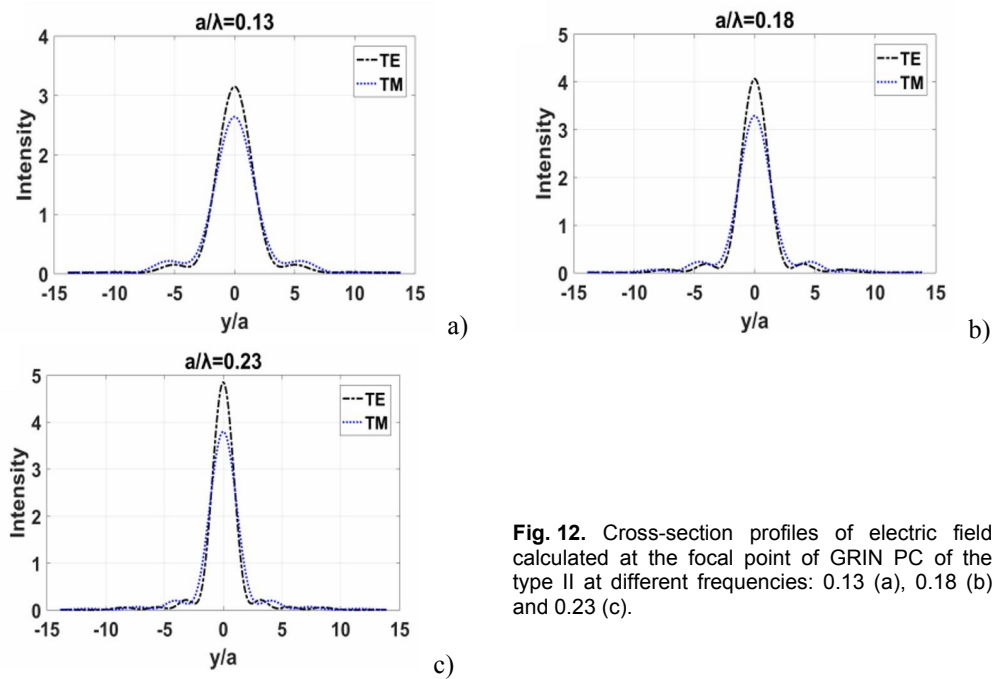
Fig. 12. Cross-section profiles of electric field calculated at the focal point of GRIN PC of the type II at different frequencies: 0.13 (a), 0.18 (b) and 0.23 (c).

The above results show that the field intensity peak becomes higher when the normalized frequency of the incident beam increases. Moreover, the field intensity for the TE polarization is higher than that for the TM polarization for each of the frequencies. The field intensity reaches its maximum and the FWHM becomes the smallest for the case $a/\lambda = 0.23$ and the TE polarization. This is the best result achieved with the structure of the type II.

3. Conclusion

In the present work we have suggested two different GRIN PC structures referred to as the structures of the types I and II. Using the plane-wave expansion approach, we have demonstrated that rotation of the air-filled ellipses in the unit cell of the structure can efficiently generate a gradient of the refractive index, despite the filling fraction is kept unchanged. This solution corresponds to the structure of the type I. In particular, we have calculated the relevant transmission optical spectrum as functions of the ellipticity and the optical index. The focusing characteristics have also been studied depending on the ellipticity variations. In fact, the paramount feature of the above solution is that the focusing effect is achieved with no structural modifications. The other type of the GRIN PC structures we have introduced is based upon modification of the filling fraction of elliptical air holes. The simulation results obtained by us for this case have demonstrated that the corresponding structure of the type II works as a focusing lens, too. It reveals a strong focusing effect for both the TE and TM polarizations.

Acknowledgments

References

1. Yablonovitch E, 1987. Inhibited spontaneous emission in solid-state physics and electronics. Phys. Rev. Lett. **58**: 2059.

2. John S, 1987. Strong localization of photons in certain disordered dielectric superlattices. Phys. Rev. Lett. **58**: 2486.

3. Lončar M, Vučković J and Scherer A, 2001.Methods for controlling positions of guided modes of photonic-crystal waveguides, J. Opt. Soc. Amer. B. **18**: 1362–1368.

4. Kurt H and Citrin D S, 2007. Photonic-crystal heterostructure waveguides. IEEE J. Quant. Electron. **43**: 78–84.

5. Zhou W D, Sabarinathan J, Bhattacharya P, Kochman B, Berg E, Yu P C and Pang S, 2001. Characteristics of a photonic bandgap single defect microcavity electroluminescent device, IEEE J. Quant. Electron. **37**: 1153–1160.

6. Luo C, Johnson S G, Joannopoulos J and Pendry J, 2002. All-angle negative refraction without negative effective index. Phys. Rev. B. **65**: 201104.

7. Kosaka H, Kawashima T, Tomita A, Notomi M, Tamamura T, Sato T and Kawakami S, 1998. Superprism phenomena in photonic crystals. Phys. Rev. B. **58**: R10096.

8. Amet J, Baida F I, Burr G W and Bernal M P, 2008. The superprism effect in lithium niobate photonic crystals for ultra-fast, ultra-compact electro-optical switching. Photon. Nanostr. **6**: 47–59.

9. Kosaka H, Kawashima T, Tomita A, Notomi M, Tamamura T, Sato T and Kawakami S, 1999. Self-collimating phenomena in photonic crystals. Appl. Phys. Lett. **74**: 1212–1214.

10. Kim T T, Lee S G, Park H Y, Kim J E and Kee C S, 2010. Asymmetric Mach-Zehnder filter based on self-collimation phenomenon in two-dimensional photonic crystals. Opt. Express. **18**: 5384–5389.

11. Centeno E and Cassagne D, 2005. Graded photonic crystals. Opt. Lett. **30**: 2278–2280.

12. Centeno E, Cassagne D and Albert J P, 2006. Mirage and superbending effect in two-dimensional graded photonic crystals. Phys. Rev. B. **73**: 235119.

13. Turduev M, Oner B, Giden I and Kurt H, 2013. Mode transformation using graded photonic crystals with axial asymmetry. J. Opt. Soc. Amer. B. **30**: 1569–1579.

14. Oner B B, Turduev M, Giden I H and Kurt H, 2013. Efficient mode converter design using asymmetric graded index photonic structures. Opt. Lett. **38**: 220–222.

15. Yilmaz D, Giden I H, Turduev M and Kurt H, 2013. Design of a Wavelength selective medium by graded index photonic crystals. IEEE J. Quant. Electron. **49**: 477–484.

16. Le Roux X, Caer C, Marris-Morini D, Izard N, Vivien L and Cassan E, 2011. Wavelength demultiplexer based on a two-dimensional graded photonic crystal. IEEE Photon. Tech. Lett. **23**: 1094–1096.

17. Kurt H, Oner B B, Turduev M and Giden I H, 2012. Modified Maxwell fish-eye approach for efficient coupler design by graded photonic crystals. Opt. Express. **20**: 22018–22033.

18. Turduev M, Giden I H and Kurt H, 2015. Design of flat lens-like graded index medium by photonic crystals: Exploring both low and high frequency regimes. Opt. Commun. **339**: 22–33.

19. Feng S, Li Z Y, Feng Z F, Cheng B Y and Zhang D Z, 2005. Imaging properties of an elliptical-rod photonic-crystal slab lens. Phys. Rev. B. **72**: 075101.

20. Ren K and Ren X, 2011. Controlling light transport by using a graded photonic crystal. Appl. Opt. **50**: 2152–2157.

21. Ren K and Ren X, 2012. Y-shaped beam splitter by graded structure design in a photonic crystal. Chin. Sci. Bull. **57**: 1241–1245.

22. Cabuz A I, Centeno E and Cassagne D, 2004. Superprism effect in bidimensional rectangular photonic crystals, Appl. Phys. Lett. **84**: 2031–2033.

23. Xu Y, Chen X J, Lan S, Guo Q, Hu W and Wu L J, 2008. The all-angle self-collimating phenomenon in photonic crystals with rectangular symmetry, J. Opt. A. **10**: 1–5.

24. Ogawa Y, Omura Y and Iida Y, 2005. Study on self-collimated light-focusing device using the 2-D photonic crystal with a parallelogram lattice. J. Lightwave Technol. **23**: 4374–4381.

25. GaoD, Zhou Z and Citrin D S, 2008. Self-collimated waveguide bends and partial bandgap reflection of photonic crystals with parallelogram lattice. J. Opt. Soc. Amer. A. **25**: 791–795.

26. Turduev M, Giden I H and Kurt H, 2013. Extraordinary wavelength dependence of self-collimation effect in photonic crystal with low structural symmetry. Photon. Nanostr. **11**: 241–252.

27. Kurt H, Turduev M and Giden I H, 2012. Crescent shaped dielectric periodic structure for light manipulation. Opt. Express. **20**: 7184–7194.

28. Giden I H, Eti N, Rezaei B and Kurt H, 2016. Adaptive graded index photonic crystal lens design via nematic liquid crystals. IEEE. J. Quantum. Electron. **52**: 1–7.

29. Trifonov T, Marsal L F, Rodriguez A, Pallares J and Alcubilla R, 2004. Effects of symmetry reduction in two-dimensional square and triangular lattices. Phys. Rev. B. **69**: 235112.

Gharaati A. and Miri N. 2017. Comprehensive analysis of two different graded-index photonic-crystal lenses. Ukr.J.Phys.Opt. **18**: 109 – 119

Анотація: *Досліджено два альтернативні підходи до реалізації градієнтних фотонно-кристалічних (ФК) структур, яким притаманний ефект фокусування. Градієнт показника заломлення досягають з використанням підходу пониження симетрії (структура типу I) або шляхом зміни коефіцієнта заповнення елементів ФК (структура типу II). Першу структуру досліджено для частот, розміщених усередині першої та другої смуг дисперсійної діаграми. Виявлено, що ефект фокусування другої структури для частот, розміщених вище забороненої зони, сильніший, аніж для частот, нижчих за заборону зону. Показано, що зміни коефіцієнта заповнення еліптичних повітряних отворів у структурі типу II формують градієнтну лінзу, яка виявляє яскраво виражений ефект фокусування. Виконано порівняння характеристик фокусування останньою структурою для світла з поляризаціями ТЕ і ТМ. Обидві структури, запропоновані в цій роботі, можуть працювати в досить широкосмуговій області.*